ISSN 1063-7842, Technical Physics, 2012, Vol. 57, No. 5, pp. 693–696. © Pleiades Publishing, Ltd., 2012.
Original Russian Text © M.V. Ivanchenko, V.A. Gritsenko, A.V. Nepomnyashchii, A.A. Saranin, 2012, published in Zhurnal Tekhnicheskoi Fiziki, 2012, Vol. 82, No. 5, pp. 115–119.

SURFACE, ELECTRON AND ION EMISSION

Enhancement of the Electron-Stimulated Desorption from Amorphous Aluminum Oxide Films on Silicon during an Increase in the Substrate Temperature

M. V. Ivanchenko[a, c]*, V. A. Gritsenko[b], A. V. Nepomnyashchii[a], and A. A. Saranin[a]

[a] *Institute of Automatics and Control Processes, Far East Branch, Russian Academy of Sciences, ul. Radio 5, Vladivostok, 690041 Russia*
**e-mail: maxim@iacp.dvo.ru*
[b] *Institute of Semiconductor Physics, Siberian Branch, Russian Academy of Sciences, pr. Akademika Lavrent'eva 13, Novosibirsk, 630090 Russia*
[c] *Far Eastearn Federal University, ul. Sukhanova 8, Vladivostok, 690950 Russia*

Received August 5, 2011

Abstract—The effect of high-temperature electron-stimulated desorption (ESD) from 20-nm-thick Al_2O_3 films deposited onto silicon wafers is studied. The ESD effect is found to be significantly enhanced upon heating. The films are found to fail before the appearance of pure Al during electron beam irradiation of a heated wafer. This process is accompanied by the formation of islands and almost pure silicon surface regions at a certain critical irradiation dose. Outside the irradiation zone, a 20-nm-thick Al_2O_3 film remains continuous even upon heating to 700°C and holding for 90 min. The effect of the primary electron beam energy on ESD from a 20-nm-thick Al_2O_3 film on silicon is investigated, and the parameters at which ESD takes place or absent are determined.

DOI: 10.1134/S1063784212050155

1. INTRODUCTION

The main trend in the evolution of the silicon technology is an increase in the speed and information capacity of devices. According to Moore's law, the latter parameter increases approximately twofold every 2 years, which is achieved mainly by scaling, i.e., a decrease in the integrated circuit device sizes. In the last four decades, the gate insulator capacitance was increased due to a decrease in the thickness of thermal silicon oxide SiO_2, whose permittivity is $\varepsilon = 3.9$. At a design standard of 63 nm, the gate silicon oxide thickness is 1.2 nm and cannot be decreased further because of unacceptably high tunnel leakage currents.

The main approach to solving this problem consists in the replacement of gate SiO_2 by high-ε dielectrics, such as Al_2O_3 ($\varepsilon \approx 10$), HfO_2, and ZrO_2 ($\varepsilon \approx 25$). The physical thickness of a dielectric can be increased and a tunnel current can be suppressed due to a high value of ε. The second important application of high-ε dielectrics consists in their use in memory cell capacitors in random-access memory. The third application of high-ε dielectrics is related to their use in memory transistors in flash memory, which is a rapidly growing segment of the silicon device market [1].

The application of high-ε dielectrics is restricted by relatively high leakage currents, which are caused by defects. Such defects in amorphous aluminum oxide are represented by oxygen vacancies [2, 3], and crystallite boundaries are likely to be such defects in polycrystalline HfO_2 films. Although aluminum oxide has a relatively low permittivity, its advantage consists in an amorphous structure, i.e., the absence of crystallite boundaries. From a technological viewpoint, it is very important to form dielectrics with the minimum number of undesirable types of defects. On the other hand, it is important to create metallic structures on the surface of such dielectrics (wires, individual clusters, etc.) by the simplest and cheapest method in order to form inexpensive memory devices and electric connections in various devices, i.e., to control a technological process. For example, it is known that ion irradiation of zirconium oxide [4] and hafnium oxide [5] causes vacancies (polyvacancies) in them and metal enrichment of the films. A similar electron irradiation effect, namely, electron-stimulated desorption (ESD), is known; it was detected during the irradiation of the surfaces of many dielectrics, in particular, alkali metal halides and some oxides, by an electron beam (see, e.g., [6]). The authors of [7] detected enhanced ESD at a high temperature by studying thin suspended films of single-crystal sapphire (α-Al_2O_3) by high-resolution transmission electron microscopy (TEM) with high-energy 100- and 200-keV beams. However, both aluminum oxide films on a copper substrate [8] and a sapphire foil with a Pt metallic contact on its rear side [9] that were irradiated by an electron beam exhibited partial suppression of the formation of metallic Al at high (HT) and room (RT) temperatures, respectively.

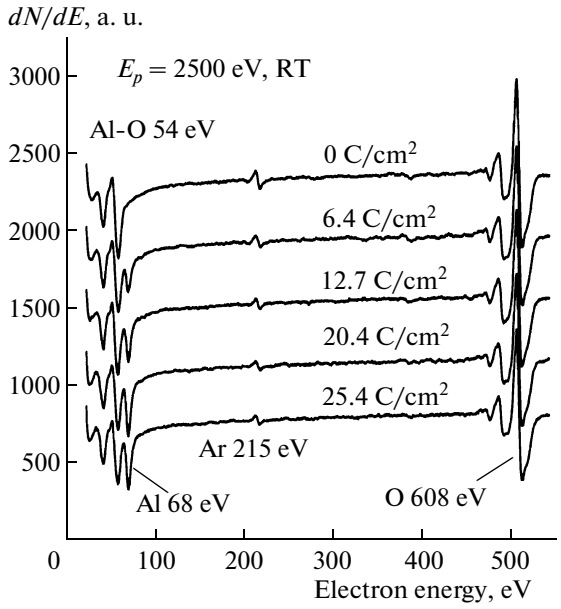

Fig. 1. Auger spectrum of an Al_2O_3 film after its ion bombardment cleaning and the Auger spectra of this film after electron irradiation at an energy E_p = 2500 eV. $T \approx$ 300 K.

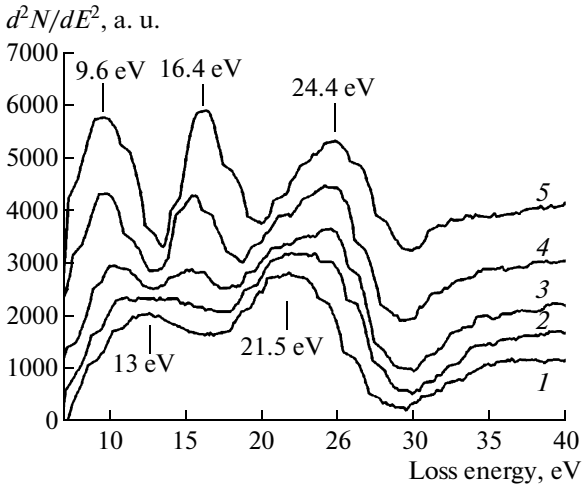

Fig. 2. Evolution of EELS spectra recorded at a primary electron beam energy of 1000 eV. The irradiation dose is (*1*) initial surface, (*2*) 2.0, (*3*) 5.1, (*4*) 10.2, and (*5*) 20.4 C/cm^2.

In addition, many works show that the ESD efficiency depends on the electron energy; however, there is no generally accepted opinion about the conditions that result in an increase or decrease in ESD when standard electron guns are used. Note that, although many works deal with ESD in dielectric films on various substrates at RT, only a few of them analyze the temperature stability of both the ESD-assisted metallic structure and initial dielectric films at HT.

The purpose of this work is to study the effect of electron irradiation on the chemical composition of amorphous aluminum oxide 20-nm-thick films deposited onto a silicon substrate and to study the conditions required for an increase or decrease in the ESD effect.

2. EXPERIMENTAL

Aluminum oxide Al_2O_3 20-nm-thick films were prepared by atomic-layer deposition from aluminum trimethyl $Al(CH_3)_3$ and water vapors H_2O, as described in [2]. As substrates, we used *p*-type (100) silicon wafers with a resistivity of 10 Ω cm. The film thickness was determined with ellipsometry. The Al_2O_3 films were amorphous, as was determined by electron diffraction.

Ion irradiation and ESD experiments were carried out in an ultrahigh-vacuum Riber LAS-600 setup with a base pressure of 2×10^{-10} Torr, which can be used to perform Auger electron spectroscopy (AES) and electron-energy loss spectroscopy (EELS). Silicon wafers with a deposited aluminum oxide film were loaded into an ultrahigh-vacuum chamber and subjected to in situ cleaning by a 500-eV Ar^+ ion beam. AES showed that, when etched by an Ar^+ ion beam, the surface had no carbon or other foreign impurities and contained a low concentration of introduced Ar. Auger spectra demonstrated that etching with an ion beam at the chosen energy did not result in the peak of metallic Al.

After preparation, samples were removed from the vacuum chamber and analyzed with a Hitachi S-3400N scanning electron microscope (SEM), and well resolved irradiated regions were examined by atomic force microscopy (AFM) on a PNI NANO-DST device.

3. RESULTS AND DISCUSSION

3.1. ESD Kinetics

Figure 1 shows the Auger spectrum of the initial Al_2O_3 film after its ion bombardment cleaning and the Auger spectra of this film after electron irradiation at an energy E_p = 2500 eV. The Auger spectrum of the initial film has an Al(*L*)O(*LL*) peak at an energy of 54 eV, which characterizes aluminum oxide, oxygen peak O(*KLL*) at 508 eV, and argon peak Ar(*LMM*) at 215 eV. Carbon contaminations are almost absent on the film surface. When the irradiation dose increases, peak Al(*LVV*) at 68 eV, which characterizes pure Al, appears and begins to grow, and peaks Al(*L*) at 54 eV and O(*KLL*) at 508 eV degrade.

Figure 2 shows the evolution of the EELS spectra recorded in the d^2N/dE^2 mode at a primary beam energy of 1000 eV. The spectrum of the initial surface has peaks at energies of 13 and 21.5 eV. During irradiation, the peak intensities decrease gradually and peaks at energies of 9.6, 16.4, and 24.4 eV appear. According to [10, 11], the peak at 13 eV is characteristic of the pure nonirradiated Al_2O_3 surface and the

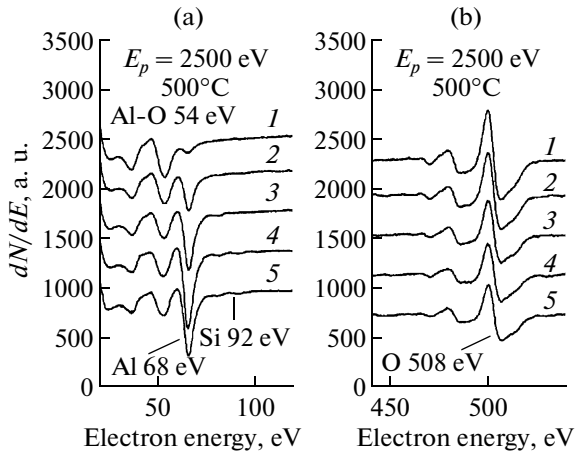

Fig. 3. AES spectra of the Al_2O_3 surface after irradiation by an electron beam with an energy E_p = 2500 eV at a substrate temperature T_s = 500°C. The irradiation dose is (*1*) initial surface, (*2*) 4.5, (*3*) 11.8, (*4*) 19.7, and (*5*) 27.6 C/cm^2.

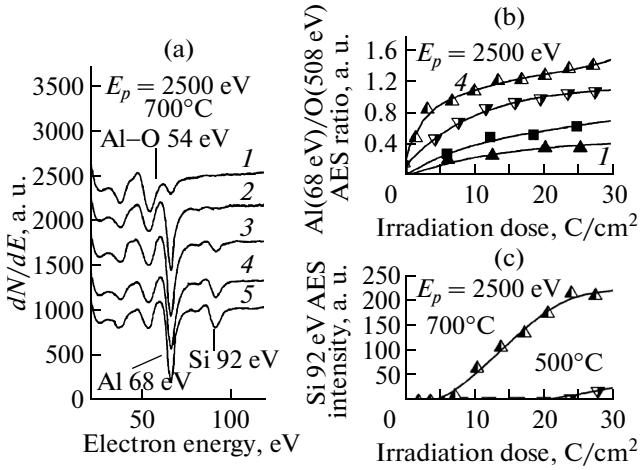

Fig. 4. (a) AES spectra of the Al_2O_3 surface after irradiation by an electron beam with an energy E_p = 2500 eV at a substrate temperature T_s = 700°C. The irradiation dose is (*1*) initial surface, (*2*) 4.5, (*3*) 11.8, (*4*) 19.7, and (*5*) 27.6 C/cm^2. (b) Dose dependences of the ratio of Auger peaks Al(*LVV*) (68 eV)/ O(*KLL*) (508 eV) at a temperature of (*1*) RT, (*2*) 300, (*3*) 500, and (*4*) 700°C. (c) Dose dependence of Auger peak Si(*LVV*) (92 eV) on the irradiation dose at a temperature of 500 and 700°C.

peak at 21.5 eV is the bulk plasmon of Al_2O_3. The peak at 9.6 eV is the surface plasmon of metallic Al: within the limits of experimental error, this energy is close to the value (10.4 eV) given in [12] for an Al film 2 monolayers (MLs) thick deposited onto Si(111)7 × 7. The peak at 24.4 eV is associated with irradiated Al_2O_3, and the peak at 16.4 is attributed to the bulk plasmon of Al (in [12], this value is 15.2 eV for a 2-ML-thick Al film deposited onto Si(111)7 × 7).

Thus, electron irradiation of the Al_2O_3 films formed by atomic-layer deposition leads to ESD of oxygen and the reduction of metallic aluminum, which is evidenced by the appearance of Auger peak Al(*LVV*) at 68 eV and the plasma loss peaks of the EELS spectra at energies of 9.6 and 16.4 eV. The process rate weakly depends on electron energy in the range 1000–2500 eV. The ESD effect is very weak at an electron energy of 200 eV.

3.2. Enhancement of ESD in Heating

An increase in the substrate temperature during electron irradiation results in a significant increase in the oxygen ESD rate. Figure 3 shows the Auger spectra recorded at a substrate temperature of 500°C and various irradiation doses of Al_2O_3. It is seen that the rate of change of the peak intensity increases noticeably as compared to this process at RT (cf. with Fig. 1). Peak Al(*LVV*) at 68 eV appears when the first spectrum is recorded and its intensity grows with the irradiation dose much faster than at RT. The peak Al(*L*)O(*LL*) 54 eV and O(*KLL*) 508 eV intensities decrease with increasing irradiation dose faster than at RT. As compared to the process at RT, the process at 500°C is characterized by the appearance of silicon peak Si(*LVV*) at 92 eV and high irradiation doses.

A further increase in the temperature leads to a further increase in the ESD rate, almost complete disappearance of peak Al(*L*)O(*LL*) at 54 eV, and a noticeable peak Si(*LVV*) intensity at high irradiation doses (Fig. 4a).

Figure 4b shows the dose dependences of the ratio of Auger peaks Al(*LVV*) 68 eV/O(*KLL*) 508 eV at temperatures of RT, 300, 500, and 700°C (curves *1–4*, respectively). This ratio is seen to increase with both the irradiation dose and the substrate temperature.

Figure 4c shows the dose dependence of the Auger peak Si(*LVV*) 92 eV intensity at temperatures of 500 and 700°C, i.e., the temperatures at which this peak was detected. At 500°C, this peak appears at a high irradiation dose and changes more weakly with the irradiation dose. At 700°C, the peak appears at a significantly lower irradiation dose and its intensity grows rapidly and levels off at an irradiation dose of 23 C/cm^2.

Figure 5a shows SEM data for the samples irradiated under the maximum ESD effect conditions, i.e., at 700°C. The irradiated region looks like a bright spot with diffuse edges. A high-resolution SEM investigation demonstrates that this spot consists of individual grains whose structure cannot be resolved. Based on our results and the data in [7–9], we assume that these grains consist of metallic Al. On the whole, the grain density and sizes correlate well with the density and sizes of the islands observed by AFM (tapping mode) in scanning of the film surface (Fig. 5b). The island density increases from the periphery of the irradiated region (Fig. 5b, left upper corner) toward the center.

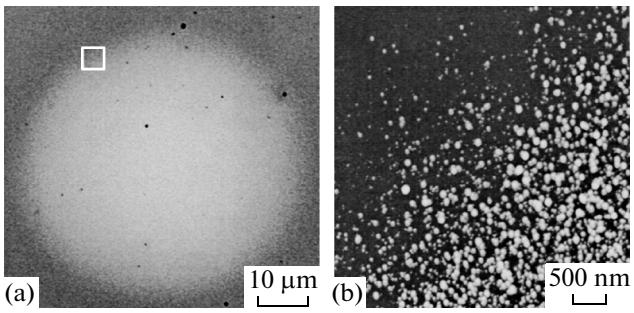

Fig. 5. (a) SEM image of the irradiated region as a bright spot. This region was formed upon irradiation by an electron beam for 90 min at a substrate temperature T_s = 700°C. The white square indicated the AFM scanning zone. (b) AFM image (tapping mode) of the left upper edge of the irradiated zone. The island density increases from the periphery of the irradiated zone (left upper corner) toward the center.

Most islands have a diameter of 50 nm and a height of 10 nm.

In the nonirradiated region, such islands and grains detected by SEM inside the irradiated region are absent. It should be noted that AES data obtained even upon heating to 700°C and holding for 90 min did not exhibit the silicon peak outside the irradiated region: the Auger spectrum was identical to that of the initial nonirradiated surface. Along with the SEM and AFM data, this finding is evidence that the 20-nm-thick Al_2O_3 film remains continuous under these annealing conditions when not subjected to electron irradiation.

CONCLUSIONS

The RT ESD effect in 20-nm-thick Al_2O_3 films deposited onto a silicon wafer was studied. The ESD effect was shown to increase substantially during heating and with the heating temperature. The film was found to fail before the appearance of pure Al during electron beam irradiation of a heated wafer. AES data demonstrate that Al islands and pure silicon surface regions form under these conditions. Outside the irradiation zone, a 20-nm-thick Al_2O_3 film remains continuous even upon heating to 700°C and holding for 90 min. We studied the effect of the primary electron beam energy on the ESD effect in a 20-nm-thick Al_2O_3 film on silicon and found that the process rate weakly depends on the electron energy in the range 1000–2500 eV and that ESD is very weak at an electron energy of 200 eV.

SPELL OK

ACKNOWLEDGMENTS

This work was supported by integration project no. 09-II-SO-02-003 of the Far Eastern and Siberian Branches, Russian Academy of Sciences; project no. 12-III-A-02-010 of the Far Eastern Branch, Russian Academy of Sciences; and the integration project no. 70 of the Siberian Branch, Russian Academy of Sciences.

REFERENCES

1. T. V. Perevalov and V. A. Gritsenko, Phys. Usp. **53**, 561 (2010).
2. T. V. Perevalov, O. E. Tereshenko, V. A. Gritsenko, V. A. Pustovarov, A. P. Yelisseyev, Ch. Park, J. H. Han, and Ch. Lee, J. Appl. Phys. **108**, 013501 (2010).
3. Yu. N. Novikov, V. A. Gritsenko, and K. A. Nasyrov, JETP Lett. **89**, 506 (2009).
4. C. Morant, J. M. Sanz, and L. Galan, Phys. Rev. B **45**, 1391 (1992).
5. A. A. Sokolov, A. A. Ovchinnikov, K. M. Lysenkov, O. E. Marchenko, and E. O. Filatova, Tech. Phys. **55**, 1045 (2010).
6. F. Golek and E. Bauer, Surf. Sci. **365**, 547 (1996).
7. C. L. Chen, H. Furusho, and H. Mori, Philos. Mag. Lett. **90**, 715 (2010).
8. A. Rar and M. Yoshitake, Jpn. J. Appl. Phys. **39**, 4464 (2000).
9. C. L. Chen, K. Arakawa, and H. Mori, Scr. Mater. **63**, 355 (2010).
10. A. Hoffman and P. J. K. Paterson, Surf. Sci. **352–354**, 993 (1996).
11. A. Hoffman and P. J. K. Paterson, Appl. Surf. Sci. **93**, 301 (1996).
12. Y. W. Chung, W. Siekhaus, and G. Somorjai, Phys. Rev. B **15**, 959 (1977).

Translated by K. Shakhlevich